

TOWARDS A TRULY BIOMIMETIC OLFACTORY MICROSYSTEM: AN ARTIFICIAL OLFACTORY MUCOSA

J.A. Covington*, S.L. Tan*, T.C. Pearce[†], A. Hamilton[°] and J.W. Gardner*

*School of Engineering, University of Warwick, Coventry, CV4 7AL, UK Email: J.A.Covington@warwick.ac.uk

[†]Department of Engineering, University of Leicester, University Road, Leicester, LE1 7RH, UK

[°]School of Electronic and Electrical Engineering, University of Edinburgh, Mayfield Road, Edinburgh, EH9 3JL, UK

Keywords: chemical sensors, electronic nose, micro-stereolithography.

Abstract

Today, the capability of the human olfactory system is still, in many ways, superior to that of artificial detection or the so-called electronic nose. Although electronic noses are often compared to their biological counterpart, they neither mimic its complex neural architecture nor achieve its performance in discriminating between complex odours. Recent developments in our understanding of the human olfactory system suggest that the olfactory mucosa (the lining of the nasal cavity comprising a mucous layer and the olfactory epithelium) behaves like a gas chromatograph. Thus receptor cells distributed beneath the mucous layer (within the olfactory epithelium) provide both spatial and temporal chemosensory information. Here we report on the development of an artificial olfactory microsystem that replicates the basic structure of the olfactory mucosa. Our system employs an 80 element chemoresistive microsensor array fabricated on a 10 mm × 10 mm silicon die. The microsensors possess carbon black/polymer nanocomposite films as the odour-sensitive elements. In addition, a micro-fluidic package has been fabricated by micro-stereolithography, with an integrated channel to act as the nasal cavity (channel dimensions 500 μm × 500 μm × 2.4 m). This channel has been coated with Parylene C, as the retentive layer, in order to mimic the partitioning mucous layer of the olfactory mucosa. The fluidic package has been placed directly on top of the sensor array and has evenly spaced openings along the channel that encompass blocks of 5 sensing elements. Results show that this biomimetic system yields both spatial and temporal odour signals, with a temporal chemical retention period of up to 110 seconds. Data analysis has revealed improvements in its ability to discriminate between two simple odours and a set of complex odours (i.e. essential oils). We conclude that closer emulation of the olfactory mucosa and nasal cavity could yield better odour discrimination and hence be superior to existing electronic nose technologies.

1. Introduction

The sense of smell is the least understood of our five human senses. Olfaction itself is of great importance to many species and is used for navigation, food sourcing and sexual

reproduction [1]. The sense of smell has been extensively studied over the past 40 years, although it is only recently that the underlying sensory mechanisms are becoming better understood [2]. Artificial olfaction has been with us since the early 1980s, although the term “Electronic nose”, or e-nose, was only defined as recently as 1994 by Gardner and Bartlett. Such systems try not to identify specific chemicals within a complex odour, for example coffee is made up of over 1,000 headspace compounds, but more to classify the type of aroma. E-noses typically combine an array of chemical sensors with overlapping sensitivities. Hence each sensor responds to a broad range of chemical components within an odour, e.g. ketones. Identification is possible due to the differences between complex odours in the concentration and mixture of chemical components. Consequently the sensors produce a response profile, or chemical fingerprint, which can be matched to a specific odour. The identification process is usually performed with some form of statistically based multivariate method or non-parametric neural network. Such systems are used regularly in, for example, environmental testing and food quality [3].

Even with the success of many e-nose systems their performance, in terms of odour concentration, identification and discrimination still lags behind that of the human olfactory system. It is generally believed that this is due to the lower complexity of e-noses when compared to their biological counterparts. For example the human olfactory system contains some 100 million olfactory receptors with approximately 350 different types of receptor binding proteins, distributed along the olfactory epithelium (the lining of the nose and part of the olfactory mucosa). In contrast e-nose systems typically have 32 or less chemical sensors in a basic chamber. Studies of the biological system have shown that the combination of the olfactory nasal cavity with the olfactory mucosa causes a “nasal chromatography” effect [3,4]. This effect is comparable to a gas chromatograph (GC). In both systems a retentive coating on the sides of the column, or nasal cavity, delay the transport of certain compounds within the odour as it traverses along the column. This delay depends upon the affinity (or partitioning) of the compound with the retentive coating. In a GC system a single sensor is used to detect the separated odour components as they elude from the end of the column. In the human olfactory system receptor cells are distributed along the olfactory pathway giving both spatial and temporal information that could, plausibly, be an important component that enhances our ability to discriminate complex odours.

Here our aim is to model and fabricate a micro-system that mimics more closely the human olfactory mucosa. By doing so it is hoped to improve e-nose systems in the discrimination and identification of odours, developing a possible new technology for low cost portable e-nose systems.

2 Artificial olfactory mucosa simulations

Before fabrication, numerous simulations were carried out to identify the optimum working conditions for promoting odour separation. A finite element model was created in FEMLAB (Ver. 2.3, Comsol, UK) to simulate the odour transport and retentive behaviour of our system. This was created instead of using a commercial GC simulation package as our model needs to model the sensors at various locations along the channel. To ensure the accuracy of our model, a commercial GC column was first modelled and the analytical solution was found to be accurate (<3% error in retention time and <9% error in separation factor).

A section of our artificial olfactory mucosa is shown in figure 1. The simulation model comprised of a 2.4 m × 0.5 mm × 0.5 mm channel with 40 sensors (5 different sensing materials) distributed along it. These sensors were placed into 8 groups of 5, with each group containing one sensor of every sensing material. The sensors in one block were separated by 20 mm and each block was separated by 150 mm, 250 mm, 280 mm, 250 mm, 280 mm, 250 mm and 150 mm. The sensors have been designated so that sensor S1 was located at 10 mm and sensor S40 was at 2260 mm along the channel. These dimensions were used in the numerical simulations. The stationary phase used in the simulations was Parylene C (poly mono-chloro-para-xylene C).

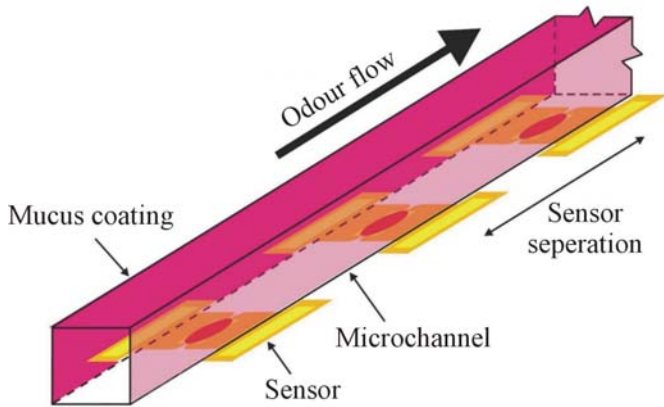


Figure 1: Section of our artificial olfactory mucosa.

Results from the simulations showed that the optimum velocity for column efficiency was 7 cm/s, although the effect of increasing flow velocity was found to be marginal on column efficiency. This velocity gives the best compromise between the unwanted broadening effect (the faster the flow the less the odour pulse front diffuses whilst traversing down the channel) and the desirable retention effect (the slower the flow rate the higher the separation of components in the odour).

On completion of these initial calculations, the outputs at the sensor locations along the channel were coupled with the sensor responses in order to model the complete system. To produce a more reliable simulation previously fabricated sensors were tested at different velocities (0 to 1600 cm/s) to pulses of ethanol and toluene vapour in air (test temperature 30±2 °C, humidity 40±5 % r.h., sensor resistance typically 2 – 8 kΩ). This was done in a micro-chamber system to help create boundary conditions for laminar plug flow. Further details covering the fabrication and test results of these sensors can be found in [5]. The sensors employed polymer/carbon black composite materials as the odour sensitive element. Here a non-conductive polymer is combined with carbon nanospheres that endow good electrical conduction to the resultant mix [6]. The sensing materials were chosen due to their rapid (ms) response time, ease of deposition, room temperature operation and the wide variety of available polymers. Five different sensor materials were tested for use in our experiments (poly(styrene-co-butadiene) (PSB), poly(ethylene glycol) (PEG), poly(caprolactone) (PCL), poly(ethylene-co-vinyl acetate) (PEVA) and poly(vinyl pyrrolidone) (PVPD), with a 20% loading by weight of carbon black). More details on the sensor materials deposition are given in section 3.1. The sensor responses were modelled using a simple first-order exponential model for both the “on” and “off” transients, given by:

$$R = R_{ON} (1 - e^{-\tau_{ON} t}) \quad (1)$$

$$R = R_{OFF} e^{-\tau_{OFF} t} \quad (2)$$

Where R is the sensor resistance, R_{ON} is the response magnitude, τ_{ON} is the response time coefficient, R_{OFF} is the decay magnitude and τ_{OFF} is the decay time coefficient. The measured parameters from the tests are given in table 1.

Sensor Type	R_{ON}	τ_{ON}	R^2
Toluene			
PSB	0.5346	0.3568	0.8638
PEVA	2.6793	0.7229	0.9626
PEG	35.1677	0.0630	0.9945
PCL	0.8580	0.103	0.9477
PVPH	2.1748	0.1887	0.9928
Ethanol			
PSB	3.3282	0.4062	0.9902
PEVA	20.9653	0.5349	0.9870
PEG	32.5009	0.1445	0.9948
PCL	7.7427	0.0807	0.9964
PVPH	2.1630	0.1881	0.9950

Table 1: Experimental results of sensor responses to ethanol and toluene vapour in air (simple odours) fitted to a first-order exponential dynamic model. R^2 is the square of the correlation coefficient.

Figure 2(a) shows profile information for a 5 s ethanol pulse (flow rate of 50 cm/s) at 5 points along the channel. As can be seen the ethanol vapour pulse broadens out as it transverses along the channel due to the diffusion effect and the retention effect of the stationary phase coating (thickness 10 μm).

Figure 2(b) shows the sensor responses at different points along the channel. The difference in retention time between sensors for each odour produces temporal signals. As different types of sensors are being used, the highly similar profiles (slowly broaden pulse) will produce very different sensor responses.

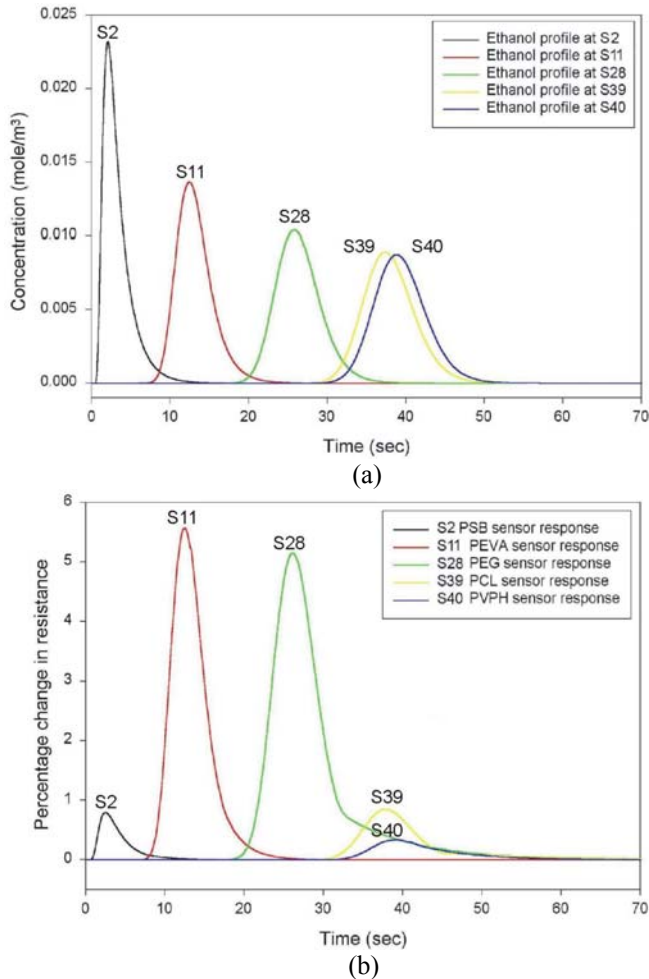


Figure 2: Simulation of (a) ethanol pulse profile along the channel and (b) sensors responses to ethanol vapour at different locations along the channel for different sensing materials.

These simulations show that it should be possible to create a system in which both spatial and temporal information can be acquired, similar to the human olfactory mucosa.

3 Artificial olfactory mucosa micro-system

On completion of the simulations, a micro-system was fabricated to further investigate these spatial-temporal signals. The micro-system comprised of a silicon-based microsensor array and a micro-fluidic package. This final micro-system was fabricated at a scale that could be used for portable e-nose systems, hence making it more applicable to real world applications. Details of these system components are given in the following sections.

3.1 Silicon based microsensor array and sensor coating

The microsensor array was fabricated using standard silicon processing techniques and then coated with polymer composite sensing materials. Each silicon die was 10 mm × 10 mm in size and contained 80 microsensors. Each sensor was formed by a pair of thin gold electrodes (20 nm chrome/200 nm gold, deposited by evaporation) deposited on top of a SiO₂ passivation layer (450 nm, deposited by thermal oxidation). The sensor elements were nominally 200 μm × 200 μm in size, with an electrode gap of 20 μm and an aspect ratio of 10. The device was finally passivated using SU-8-10 (10 μm thick layer, Microchem, UK) with openings for deposition of sensing materials and bonding. Due to the simplicity of the array only one metal layer was required for tracking. Five different polymer composite recipes were used to produce the sensing materials, as given in Table 2.

Polymer	Carbon black	Solvent
Poly styrene-co-butadiene (PSB), 0.7 g	0.175 g	Toluene, 20 ml
Poly ethylene-co-vinyl acetate (PEVA), 1.2 g	0.3 g	Toluene, 20 ml
Poly ethylene glycol (PEG), 1.2 g	0.3 g	Ethanol, 20 ml
Poly caprolactone (PCL), 1.2 g	0.3 g	Toluene, 20 ml
Poly 4-vinyl phenol (PVPH), 1.2 g	0.3 g	Ethanol, 20 ml

Table 2: Sensing materials and solvents used to coat the microsensor array.

The polymers were supplied by Sigma Aldrich (UK) and the carbon black (Black Pearls 2000) was supplied by Cabot Corporation (USA). The polymers were either in powder form or small crystals while the carbon black was supplied as nanospheres with diameters of typically 50 to 80 nm. The polymers were first dissolved in their respective solvent overnight, with the aid of a magnetic stirrer and at an elevated temperature (50 °C). Next, carbon black was added and the mixture sonicated for 10 minutes using a flask shaker (Griffin and George, UK). The mixture was then deposited onto the sensor electrodes using an airbrush (HP-BC Iwata, Japan) controlled by a micro-spraying system (RS precision liquid dispenser, UK). A beryllium copper mask was etched with 300 μm holes, using standard photolithography techniques, to aid deposition of the sensing material and to reduce the possibility of cross contamination. The sensor electrodes were aligned to the mask using an X-Y stage before deposition occurred. The airbrush was held 10 to 15 cm away from the mask and several passes were sprayed depending on the desired thickness (or resistance). This gave a circular coating of typically 300 ± 50 μm in diameter and 20 ± 5 μm thick. The electrical resistances of the sensors were controlled through the deposition process to a value of 2 kΩ to 8 kΩ. After coating, the sensor array was mounted in a 256 pin PGA package (Spectrum Semiconductor). Figure 3 shows a photograph of a fabricated microsensor array which has been coated with sensing materials.

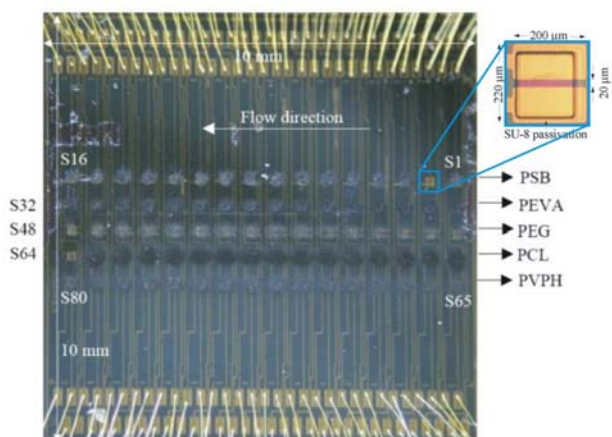


Figure 3: Photograph of a fabricated microsensor array with sensing coating. Sensor materials have been labelled and sensor numbers of S1 to S80 also defined.

3.2 Micro-fluidic package

The micro-fluidic package was fabricated using a modified Envisiontec Perfactory Mini micro-stereolithography (MSL) machine. Micro-stereolithography (MSL) is a similar process to stereolithography, which is used extensively for rapid prototyping. In an MSL system, a 3D CAD model of the object is first created, this CAD model is then sliced horizontally into a series of 2D images that represent multiple cross-sections of the 3D object. These layers are translated into appropriate control and positioning co-ordinates and are cured layer by layer (cross section by cross section) into a photocurable resin. After each layer has been cured into the resin, the object is moved vertically to allow an uncured layer of resin to cover the previously cured layer. The Perfactory MSL system employs projection-based (dynamic masking) technology. The hardware consists of a visible light source, a dynamic mask modulator (implemented using a Digital Micro-mirror Device or DMD), focusing optics, a resin tray and a Z-stage for moving the base (build platform). For each layer, the DMD modulates the light in such that the layer mask pattern appears under the resin tray. The DMD does this by flipping the mirrors toward or away from the light source. Each layer mask is stored as a mono picture file with each pixel corresponding to a mirror state. Upon exposure, the pattern corresponding to the mask cures the resin. This layer of resin is trapped between the resin tray and the build platform. Once cured, the Z-stage (driven by a lead screw and a stepper motor) moves upwards by the layer thickness step. As the surface of the resin tray is coated with a silicone-based material with lower coefficient of friction than the build platform, the cured layer will detach from the resin tray and stay attached to the build platform. Table 3 gives information on the specification of the MSL system. Typically 25 μm slices were used in the Z-direction with a build time of typically 10 seconds per slice.

A CAD drawing of the micro-fluidic package is shown in figure 4. Here the drawing has been cross-sectioned to make the internal channels visible. As can be seen in figure 4 the micro-fluidic package has been designed to contain

multiple channels, stacked in the Y direction, with openings and the top and bottom of each channel. The openings in the centre section at the bottom are designed to encompass blocks of 5 sensors. The remaining openings are there to aid cleaning of any residual resin.

System variant	Perfactory Mini SXGA (Multi Lens)
Resolution	SXGA: 1280 × 1024 pixel
Build envelope XYZ	41 × 33 × 230 mm
Pixel size XY	32 μm pixel (16 μm with ½ pixel shift)
Layer thickness Z	25 μm

Table 3: Build specification of Perfactory system.

After fabrication the micro-fluidic package was coated with a retentive layer. Here an evaporation technique using a commercial machine (PDS 2010 Labcoater™ 2 (Specialty Coating Systems, Indianapolis, USA), was used to deposit Parylene C. This material is very similar to other GC stationary phase materials with the added advantage of room temperature deposition. However, as this material is relatively new as a stationary phase, its retention characteristics have not been fully studied hence the diffusion and partition coefficients of various analytes are not available. Initial investigations show it has a similar retention characteristics to PEG [7]). The deposition is performed in a vacuum and took approximately 3½ hours to deposit a 10 μm thick layer.

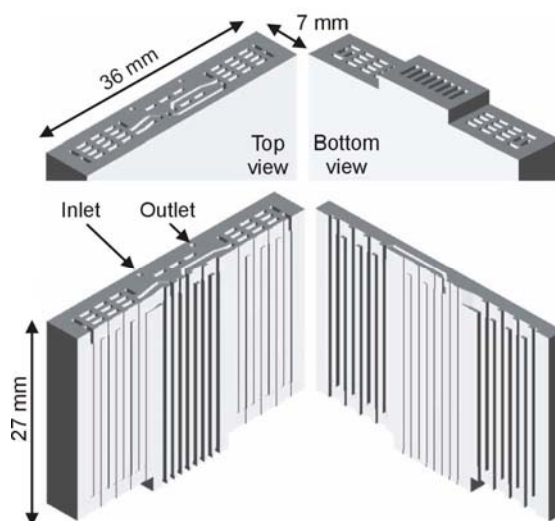


Figure 4: CAD drawing of MSL package, 2.4 m in length with channel dimensions of 0.5 mm × 0.5 mm.

Once the deposition of Parylene C was completed the holes on the top and bottom were sealed by placing a strip of plastic (also formed from MSL) over the holes. Uncured resin was used as a sealant, which cured in natural light. The package was then fitted over the sensor array, again sealed with uncured resin (resin was painted onto the underside of the package and pressed onto the sensor array). Metal pipe

fittings were finally added to the micro-package for connection to a vapour flow system. A photograph of the micro-package, after Parylene C coating, and after final assembly is shown in figure 5.

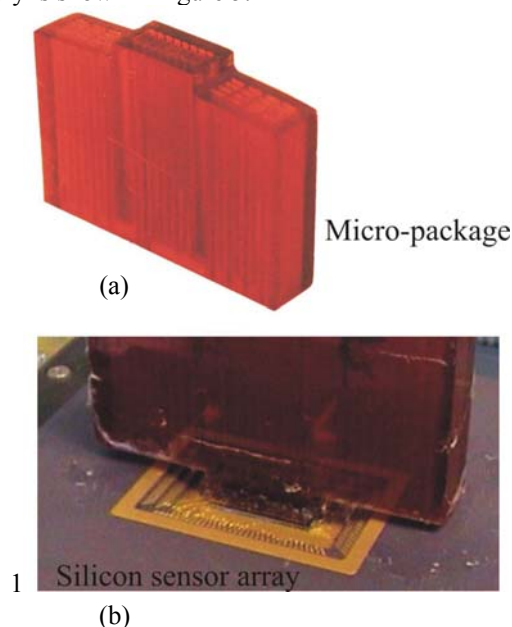


Figure 5: Photographs of (a) MSL micro-package and (b) final assembled system.

4. Experimental setup

For testing the sensor chip was connected to a custom electronic interface where each chemical sensor was used as the feedback resistor of an op-amp (OP2277, Analog Devices) in an inverting configuration. The output voltage was then sampled by on-board 16-bit ADCs (AD7805, Analog Devices) controlled through a National Instruments PC-DIO-96 and LabVIEW™ (version 6.1) control and data storage software. Finally the fluidic package was connected to a custom-made vapour flow system. This system can inject short pulses of simple and complex odours in air over the sensors at different flow rates. Further details of the test setup can be found at [8].

To evaluate our artificial olfactory mucosa, first simple odours of ethanol and toluene vapour in air were injected into the micro-fluidic system; the temperature was 30 ± 2 °C and relative humidity of 40 ± 5 % throughout all of the experiments. The carrier gas used for all the tests was laboratory air. This was done to keep all the results as close as possible to real life condition. Before each experiment the carrier gas flowed through the system for one minute to stabilise the sensor resistance. The vapour pulse was turned on at time, $t = 1$ sec and turned off at time, $t = 101$ sec to give, for example, a 100 sec pulse duration. Each test lasted for 30 minutes. Finally, a set of complex odours (i.e. milk, vanilla, peppermint and mixtures of these (50:50 ratio by volume)) were used to evaluate more meaningfully the olfactory capability of the micro-system.

5. Results

Experimental results, taken at a flow rate of 25 ml/min and 150 ml/min, show that the retentive layer causes very different delays along the micro-channel of up to 51 s and 106 s for ethanol and toluene vapour, respectively. This was calculated by comparing the time the first and last sensors (PCL coated sensors in this case) reached 50% of its maximum response value.

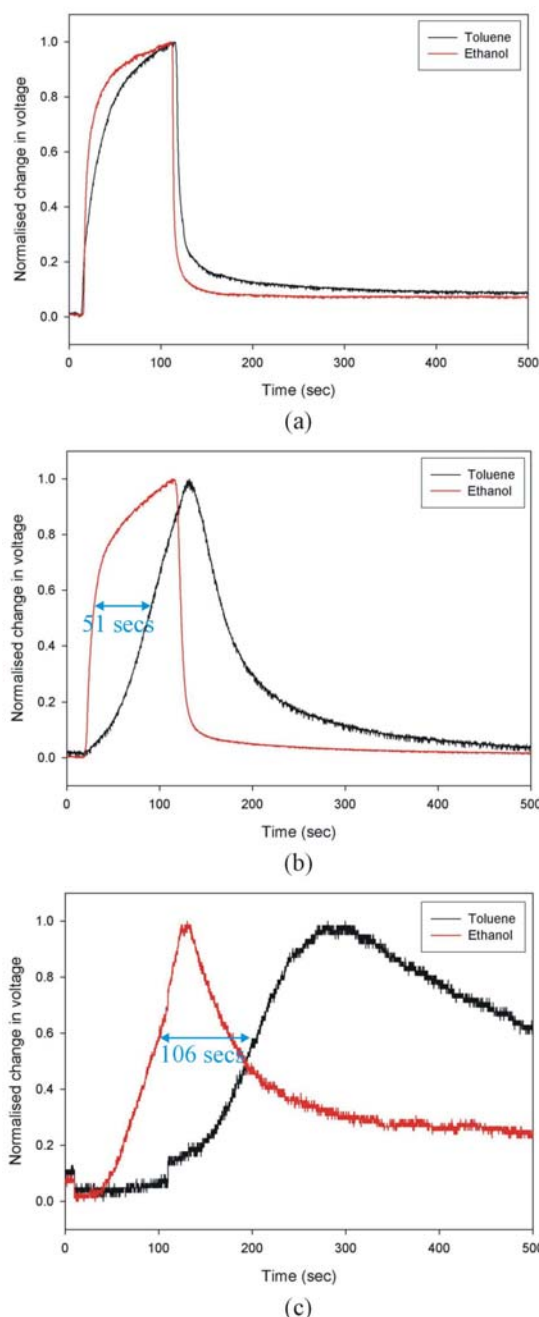


Figure 6: Varying temporal signals for simple vapours on micro-system (PEG sensors only). (a) Sensor S50 (25 mm from inlet) response. (b) Sensor S54 (900 mm from inlet) response. (c) Sensor S63 (2375 mm from inlet) response (flow rate 25 ml/min).

Figure 6 shows a comparison of sensor responses at different locations along the channel to ethanol and toluene vapour in air. For figure 6(a), both ethanol and toluene vapour pulses reach the sensor at the same time. As the pulses travel along the channel to (b), the retention effects on the two vapours become significant. Towards the outlet at (c), the two vapours pulses are partly separated, showing the micro-system is behaving like a basic GC column.

For the complex odours, the responses of 5 sensors (S34, S38, S57, S27 and S30) placed along the channel were recorded. The spatio-temporal signals for the various odours were extracted for PCA (Principal Components Analysis) to determine the viability to perform linear classification. For simplicity, the spatial signal utilised only the response magnitude (i.e. ΔV , the maximum change in output voltage) and the temporal signal used the time at which the output reached 50 % of ΔV . These experiments were conducted at a flow rate of 25 ml/min and pulse width of 25 sec with 5 replicates. Three PCAs were performed, one operated on the spatial data only, a second used the temporal data, while the third utilised the combined data (spatio-temporal data). Figure 7 shows the results of the combined data analysis, clearly showing that the test odours can be linearly separated.

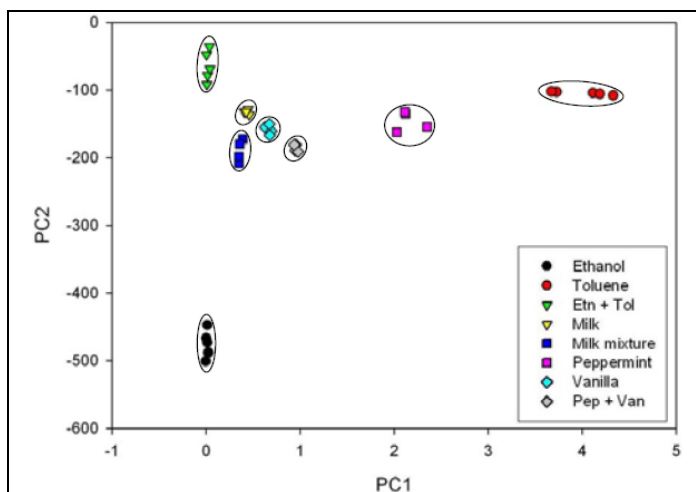


Figure 7: PCA plots with spatio-temporal data of 5 sensors (S34 (PEG sensor 30 mm from inlet), S38 (PEG sensor 1060 mm from inlet), S57 (PCL sensor 2100 mm from inlet), S27 (PEVA sensor, 2160 mm from inlet), and S30 (PEVA sensor, 2200 mm from inlet)).

It was observed that the distance between the complex odours, as represented in multivariate vector space, was greater for the spatial-temporal data than that for the spatial data or temporal data alone. The performance of the spatial data, that used in a conventional electronic nose, was also found to outperform that of the temporal data alone. Care must be taken when analysing the different datasets because of the doubling in the dimensionality of the spatio-temporal dataset and magnitude of signals. A more detailed parametric study of the responses is being carried out using both linear and non-linear classification methods, such as discriminant and radial basis function analyses. The results of this study will be published elsewhere.

Conclusions

Here we report on the first attempt to make an artificial olfactory mucosa by combining a silicon sensor array with a micro-fluidic package. This system has been designed and fabricated to exploit the nasal chromatographic phenomena, which has been observed in the human olfactory system. Our system aims to replicate this biological process by generating similar spatio-temporal signals. Here an 80 element microsensor array, with 5 different sensor tunings, has been combined with a 2.4 m long Parylene C coated channel fabricated using micro-stereolithography. The distributed microsensor system was tested with both simple and complex odours to examine its capability in generating both spatial and temporal signals. The results show that the “e-mucosa” system can generate spatio-temporal signals for both types of odours, with a temporal delay of up to 106 s. Such temporal signals, which have been shown to exist in biological olfactory system, could well be the critical factor in improving existing e-nose instruments.

Acknowledgements

We would like to thank EPSRC (grant no. GR/R37975/01) for funding this research project.

References

- [1] E.B. Goldstein, *Sensation and perception*, Sixth Edition, Wadsworth Inc Fulfilment, 2002.
- [2] L. Buck, R. Axel, “A novel multigene family may encode odorant receptors: a molecular basis for odor recognition, *Cell*”, **65**, pp. 175-187, 1991.
- [3] J.W. Gardner, P.N. Bartlett, *Electronic noses: principles and applications*, Oxford University Press, Ltd Oxford, 1999.
- [4] M. Lysetskiy, A. Lozowski, J.M. Zurada, “Invariant recognition of spatio-temporal in the olfactory system model”, *Neural Processing Letters*, **15**, pp. 225–234, 2002.
- [5] S.S.L. Tan, J.A. Covington, J.W. Gardner, “Velocity-optimised diffusion for ultra-fast polymer-based resistive gas sensors”, *IEE- Science, Measurement and Technology*, 2006 (at press).
- [6] B. Matthews, J. Li, S. Sunshine, L. Lerner, J.W. Judy, “Effects of electrode configuration on polymer carbon-black composite chemical vapour sensor performance”, *IEEE Sensor Journal*, **2**, pp. 160-168, 2002.
- [7] H.S. Noh, P.J. Hesketh, G.C. Frye-Mason, “Parylene gas chromatographic column for rapid thermal cycling”, *J. Microelectromechanical Systems*, **11**, no. 6, pp. 718-725, 2002.
- [8] S.L. Tan, “Smart chemical sensing microsystem: towards a nose-on-a-chip”, PhD thesis, School of Engineering, University of Warwick, Coventry, UK, September 2005